Temperature Induced Structural Changes in Syndiotactic Polystyrene/*cis*-Decalin Systems

T. Roels,[†] S. Rastogi,[‡] J. De Rudder,[†] and H. Berghmans*,[†]

Laboratory for Polymer Research, Catholic University Leuven, Celestijnenlaan 200F, B3001 Heverlee, Belgium, and Center for Polymers and Composites/The Dutch Polymer Institute (DPI), University of Technology, P.O. Box 513, 5600MB Eindhoven, The Netherlands

Received June 2, 1997; Revised Manuscript Received October 14, 1997[⊗]

ABSTRACT: Phase transformations in solutions of syndiotactic polystyrene in *cis*-decalin has been investigated by differential scanning calorimetry, wide and small angle X-ray scattering, and Fourier transformed infrared spectroscopy. The in-situ performed experiments enabled identification of the different modifications without solvent removal. Quenching a solution leads to formation of the helical δ-phase. On heating, this phase transforms into the planar zigzag β-phase. The transformation of the helical phase (δ) into the planar zigzag (β) during heating proceeds via a melting−recrystallization process.

Introduction

Syndiotactic polystyrene (sPS) shows a complex polymorphic behavior, strongly influenced by the sample history.[1−9] The polymer chain backbone can adopt two different conformations: an all-trans planar zigzag (T_4) and a helical structure (T_2G_2). These two different conformations give rise to four crystal modifications.[1−5] The difference in chain packing of the zigzag conformation leads to the α- and β-modifications that can be obtained from the melt or from solution. The helical conformation on the contrary can only be formed in the presence of a solvent,[1−3,10−20] and this leads to the formation of two different helical phases, the γ- and δ-phases. In addition, the possibility of the formation of two mesophases is reported.[4,20−24] Depending on the conformation that is adopted, the nomenclature "helical" mesophase and "planar" mesophase is proposed.[20]

In earlier studies the concentration dependence of the structure formation in decalin, *o*-xylene, and some chlorobenzenes has been reported.[25−28] The formation of the different phases was shown to be controlled to a large extent by kinetic factors. But the temperature−concentration phase diagrams, obtained under well-controlled experimental conditions, allowed us to conclude that the helical phase represents an incongruent melting polymer−solvent compound. The construction of these diagrams, however, was mainly based on calorimetric observations (DSC) and wide angle X-ray scattering (WAXS) measurements, using a flat film camera. This limits to an important extent the structural observations, as most of the solvent has to be eliminated in order to observe well-defined patterns. It is also evident that this drying operation can result in phase transformation because this corresponds with a shift in concentration through the phase diagram. In situ investigations of phase transformations during heating was also not possible. But such information could be very valuable and could lead to more evidence of the phase behavior and related transformation mechanisms.

Therefore, high-intensity synchrotron radiation was used together with an electronic counting device in order to observe in situ the X-ray scattering patterns simultaneously at wide and small angles, in the presence of the solvent, and investigate the relation between the temperature and crystal structure.

Combination of this technique with DSC and FTIR experiments further provided insight into the stability of the different phases and their transformation behavior.

Experimental Section

Materials. The number-average and mass-average molecular masses of the syndiotactic polystyrene used, determined by GPC in 1,2,4-trichlorobenzene, were 14.3×10^4 and 42.9×10^4 g/mol. The syndiotactic polystyrene sample was provided by Dow Chemical. *cis*-Decalin with a degree of purity of 0.99 as obtained from Aldrich Chemie was used.

Dynamic Scanning Calorimetry. A Perkin-Elmer DSC-7 was used to study thermal transitions at 5 °C/min. The polymer mass fraction, w_2, is used to express the polymer concentration.

FT Infrared Spectroscopy. A Perkin-Elmer FTIR 2000 was used. The polymer solution was put between NaCl windows. To increase the signal to noise ratio, a minimum of 32 spectra with resolution of 2 cm^{-1} are added. During heating eight scans are collected at a heating rate of 2 °C/min.

SAXS/WAXS Equipment. Simultaneous SAXS/WAXS experiments were performed on Station 8.2, Daresbury (U.K.) using a wavelength of 1.5 Å. To have better information, WAXS pattern experiments were repeated on Station ID11/BL2 of the European Synchrotron Radiation Facility (ESRF) in Grenoble, France. A flux of $>10^{12}$ photons/s at the sample position was used. The beam size at the sample was 0.2×0.2 mm^2. A wavelength of 0.757 Å was used for WAXS studies. A parallel plate ionization detector was placed in front of the sample to record the incident intensity. The detection of the scattered photons was established with a Princeton CCD detector. The solutions were enclosed in sealed capillaries.

Polyethylene single crystals were used to calibrate the WAXS detector. For calibration of the SAXS detector, the scattering pattern from an oriented specimen of wet collagen (rat-tail tendon) was used.

Results and Discussion

Phase Behavior of sPS/*cis*-Decalin. The shape of the temperature−concentration diagram is highly dependent on solvent structure and quality. The study of the crystal structure transformations necessitates a system in which the transition from the helical phase into the planar zigzag phase can take place over the whole concentration range. This can only be realized

[†] Catholic University Leuven.
[‡] University of Technology.
[⊗] Abstract published in *Advance ACS Abstracts,* December 1, 1997.

S0024-9297(97)00795-X CCC: $14.00

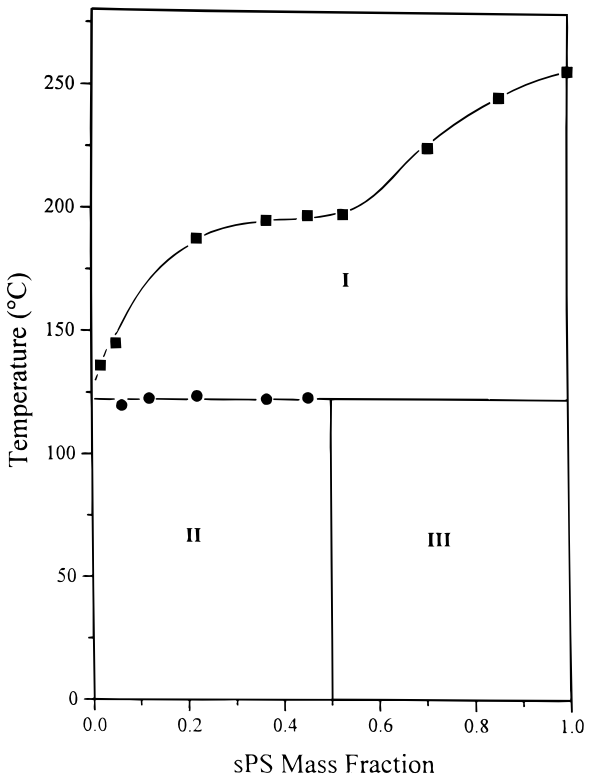

Figure 1. Temperature−concentration diagram of sPS/*cis*-decalin. (■) Melting of the zigzag phase and (●) helical phase, drawn after ref 25.

in poor solvents like *cis*-decalin. The detailed study of the phase behavior of this system has been reported in a previous paper.[25] The melting point−concentration relationship for the different phases is represented in Figure 1.

This type of diagram is characteristic for the formation of a polymer−solvent compound. Up to now, it was not possible to localize the exact composition of the compound (δ-phase). A standard technique used for small molecular compounds is the dependence of the melting enthalpy on concentration. This melting enthalpy should go through a maximum at the composition of the compound. But such a relationship supposes that the compound formation is not influenced by the overall concentration of the solution. This is certainly not the case in the system sPS−decalin. The melting enthalpy per gram sPS decreases with increasing polymer content.[25,26] Therefore the degree of crystallinity is not constant but decreasing with increasing polymer content. One can nevertheless conclude from such a temperature−concentration investigation that this composition has to be situated around $w_2 = 0.50$.[25] Therefore the composition of the compound is put in Figure 1 at that concentration. Calorimetric observations and SAXS/WAXS analysis will be performed with solutions that have an overall polymer content $w_2 = 0.40$. The optimum condition would be the concentration that corresponds exactly with the composition of the polymer solvent compound but this condition cannot be realized for reasons given earlier. A polymer concentration $w_2 = 0.40$ was chosen, close to the estimated composition of the compound and in a concentration range that still can be prepared as a homogeneous system without too much trouble. The intensity of the DSC signals and of the X-ray scattering signals will benefit from this situation.

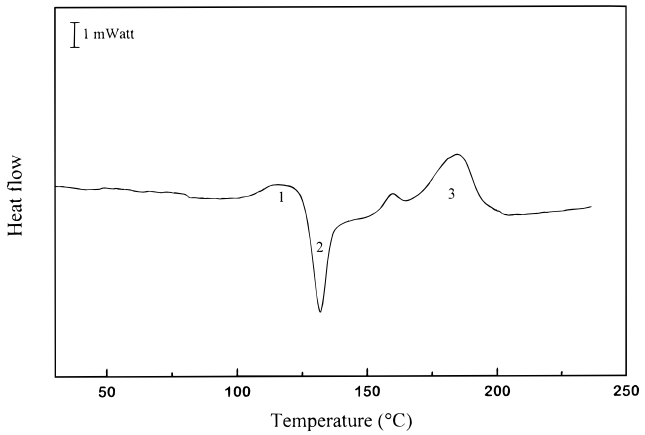

Figure 2. DSC thermogram of a sPS/*cis*-decalin solution ($w_2 = 0.40$).

In the phase diagram represented in Figure 1, three different temperature−concentration regions have to be considered.

Region I corresponds to the coexistence of a solution and the zigzag crystal phase. In region II, pure solvent coexists with the compound. In region III, the compound should coexist with the zigzag phase. But difficulties in the establishment of this equilibrium can arise from the presence of the glass transition−concentration relationship ($T_g - w_2$).

Kinetic factors also play an important role. Cooling a homogeneous solution slowly from high temperatures results in the crystallization in the zigzag phase (I). Formation of the polymer−solvent compound can only be realized by quenching.

Calorimetric Investigations of the Phase Relationships. In *cis*-decalin, the helical phase can only be formed by quenching the solution from high temperatures into concentration region II. Under these conditions, heating of the sample will result in an incongruent melting of the helical phase and a recrystallization into the zigzag phase. This transformation can easily be followed by DSC, and this is illustrated in Figure 2 for a solution with $w_2 = 0.40$. Minor differences in the melting temperatures of the planar zigzag form in comparison with the presented phase diagram are due to the higher molecular weight of the sPS used in this study. The melting and recrystallization phenomenon remains unaffected by molecular weight.

The DSC scan reveals an endothermic signal (1) immediately followed by an exotherm (2). On further heating, a second endotherm is observed (3). Most likely, endotherm 1 represents the melting of the helix phase. But this melting signal is very incomplete, as it overlaps with the recrystallization into the zigzag phase (2). This zigzag phase melts at even higher temperatures (3). The formation of this phase at a large degree of undercooling can be responsible for the multiple melting signal. These phase transitions have been followed in-situ by X-ray scattering at wide and small angles.

Structural Analysis of the Phase Transformation by SAXS and WAXS. Partially dried samples are generally used to analyze the crystal structure of the different phases. But the elimination of the solvent, however, can induce changes in this crystal structure (δ to γ or even to zigzag). Therefore the SAXS and WAXS observations were made by using polymer solutions with $w_2 = 0.40$. This high polymer content guarantees a high enough intensity of the diffraction

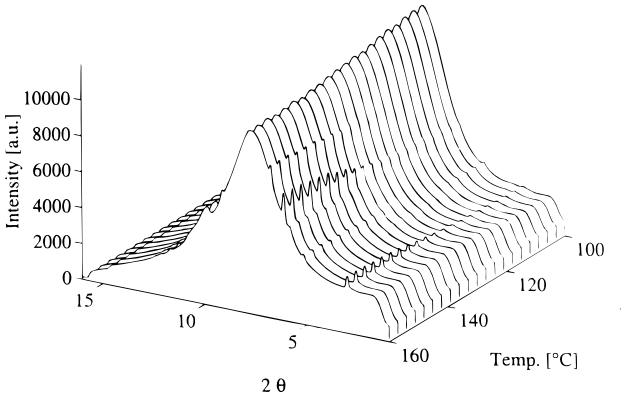

Figure 3. 3D overview of WAXS patterns during heating the sPS/*cis*-decalin solution.

Table 1. Observed 2θ Values and *d* Spacings at −10 and +160 °C and Literature Data for the δ- and β-Modifications (ref 3)

$T = -10$ °C			$T = 160$ °C		
2θ	*d* (Å)	*d*(δ) (Å)	2θ	*d* (Å)	*d*(β) (Å)
3.0	14.46		3	14.46	14.37
		11.32			
4.95	8.76	8.66			
			5.1	8.5	8.46
			6.05	7.17	7.18
6.2	6.99	6.60			
			6.65	6.53	6.52
			7.55	5.75	
8.1	5.36				
		5.21			
			9.1	4.77	4.78
					4.39
10.0	4.34	4.46			
					4.18
11.4	3.81	3.88			
			11.6	3.74	3.72
					3.58
		3.19			
					2.56

signals related to the polymer crystal structure so that they can be distinguished from the broad signal that results from the presence of a large amount of solvent. The use of sealed glass capillaries guarantees a constant polymer concentration during the thermal treatment of the samples. Quenching these samples from the solution state at high temperature into liquid nitrogen followed by heating to room temperature transforms the sample in the δ-phase. Then the SAXS and WAXS patterns were recorded as a function of temperature at 5 °C/min.

WAXS. Figure 3 represents the three-dimensional view on the evolution of the WAXS patterns in the temperature region of interest. The signals that can be ascribed to the presence of a polymer crystal structure are superimposed on the broad maximum that results from the presence of the solvent. Subtraction of the solvent signal was not performed, because the solvent plays an important role in the polymer−solvent compound. Nevertheless, positioning of the maximum of the different peaks was possible and the corresponding *d* spacings and 2θ values collected at −10 and +160 °C are reported in Table 1. This table also contains *d* spacings reported by Guerra for the β-modification (12) and for the δ-modification that have been derived from Figure 1 in ref 12.

An important change in the patterns is observed at 140 °C, and this is illustrated in Figure 4, in which the patterns recorded at −10 and +160 °C are compared.

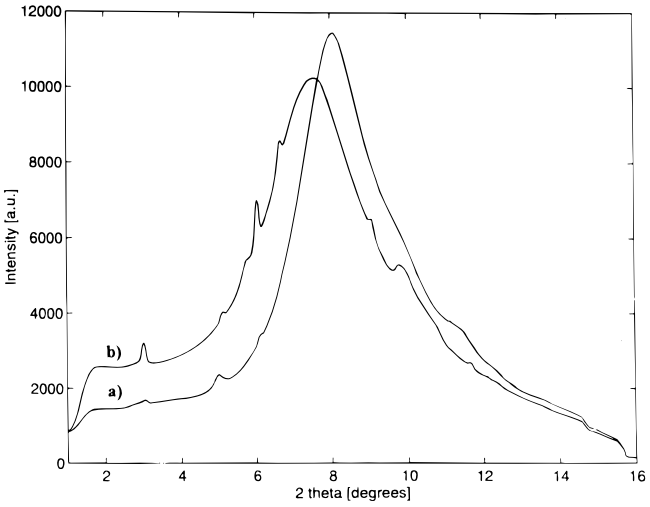

Figure 4. WAXS patterns at (a) −10 °C and (b) 160 °C.

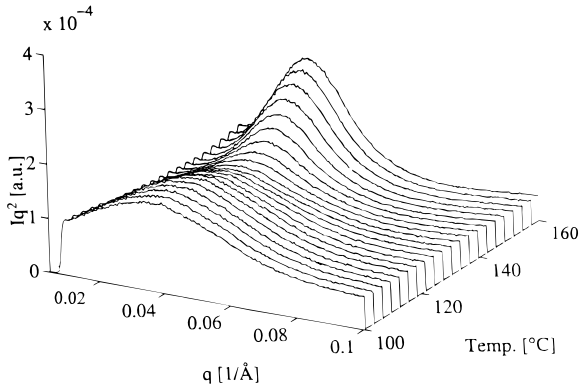

Figure 5. 3D overview of SAXS patterns during heating the sPS/*cis*-decalin solution.

The broad peak, which must be attributed to the solvent, is positioned at *d* spacings of 5.36 Å at −10 °C (2θ = 8.1°) and 5.75 Å at 160 °C (2θ = 7.55°). The maximum in the diffraction band of a solvent is related to the presence of a Van de Waals interaction between the solvent molecules. Pure *cis*-decalin shows a maximum corresponding with 5.6 Å (2θ = 7.75°) at room temperature. The shift in this maximum arises from both the temperature dependence of the position of the maximum and the structure formation in solution. This shift makes the subtraction of the contribution of the solvent difficult. The diffraction maxima characteristic for the presence of the structuralized polymer appear on top of the broad solvent signal. Below 140 °C most of the polymer is in the δ-phase with characteristic *d* spacings at 8.76 Å (2θ = 4.59°) and 3.81 Å (2θ = 11.4). The presence of a weak diffraction peak that corresponds with a *d* spacing of 14.46 Å (2θ = 3.0) is indicative of the presence of a small amount of zigzag structure. The pattern at 160 °C shows all characteristic peaks for the β-phase.

These changes in crystal structure on heating in combination with the melting−recrystallization signal observed in the DSC experiments, clearly support the earlier proposed transformation mechanism of the δ-modification into β-modification.

SAXS. SAXS experiments were performed under the same experimental conditions of sample treatment and temperature cycle. The changes in the diffraction patterns obtained in the temperature domain of interest are shown in Figure 5. A broad signal with a maximum at a *q* value of 0.035 Å^{-1} is observed in the temperature

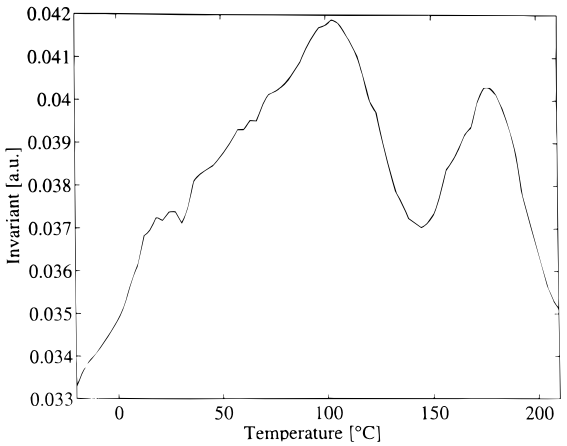

Figure 6. Invariant vs temperature during heating the sPS/*cis*-decalin solution.

region below 140 °C. Such a pattern reflects the absence of the long range order that is generally formed when crystallization with formation of folded chain lamellar structures has taken place. The supramolecular organization could very well correspond to a dense network of bundle-like structures formed by the association of helical segments. This type of morphology has already been reported for the similar system isotactic polystyrene/decalin.[29] The maximum disappears between 120 and 135 °C and a new maximum at $q = 0.03$ Å^{-1} develops when the samples reach temperatures above 140 °C. This corresponds with a d spacing of 210 Å. These changes have to be ascribed, like in the WAXS observations, to the transformation from δ-modification into the β-modification. This β-modification normally crystallizes from the melt or from solution with the formation of lamellar folded chain structures so that we can ascribe the appearance of the SAXS signal to the formation this type of structure during the melting−recrystallization process.

The observations made in both SAXS and WAXS confirm the DSC data. A good illustration and summary is given by the change in the invariant $Q = \int_0^\infty q^2 I(q)\, dq$ of the SAXS spectra as a function of temperature (Figure 6). This invariant reflects the electron density fluctuation between different regions.

Table 2. Typical IR Bands for Helical and Zigzag Conformations

helix (cm^{-1})	zigzag (cm^{-1})
1276−1277	1396
1168	1220−1224
943	902.5 (α)
571−572	911 (β)
535−537	542
548	

Thus changes occurring in the electron density fluctuations during phase transformations can be followed by Figure 6. The increase in the invariant in the temperature region −10 to +105 °C goes in parallel with the development of the δ-phase. From 105 to 150 °C, the invariant of the pattern decreases and increases again at higher temperatures. The decrease in the invariant is characteristic for the melting process where the density fluctuations between different regions nearly disappear. The following increase on heating further suggests crystallization and crystal perfecting in the β-phase as anticipated by WAXS. Thus a decrease and increase in the invariant further confirms melting and recrystallization phenomenon during the helical to planar zigzag transformation. Between 175 and 180 °C, melting of this β-phase sets in, which is in accordance with the endotherm observed around these temperatures in DSC.

Infrared Spectroscopy. The infrared absorption spectra of the different modifications of sPS have been extensively studied in the literature.[13,23,30−37] They reflect the differences in molecular conformations: helix, zigzag, and amorphous random coil conformation. The difference in crystal modification within one conformation is not showing up clearly with this spectroscopic technique. The difference between the γ- and δ-phase lies in a higher absorption intensity for the γ-phase.[31] Table 2 summarizes the useful absorption bands that distinguish the helical from the zigzag conformation, and Figure 7 shows the spectra of the *cis*-decalin (Figure 7a) and of the different conformations of the polymer chain (Figure 7b−d). No solvent subtraction was performed on the spectra taken in solution.

The spectrum of pure amorphous sPS (Figure 7d) was obtained with a sample that was quenched from the

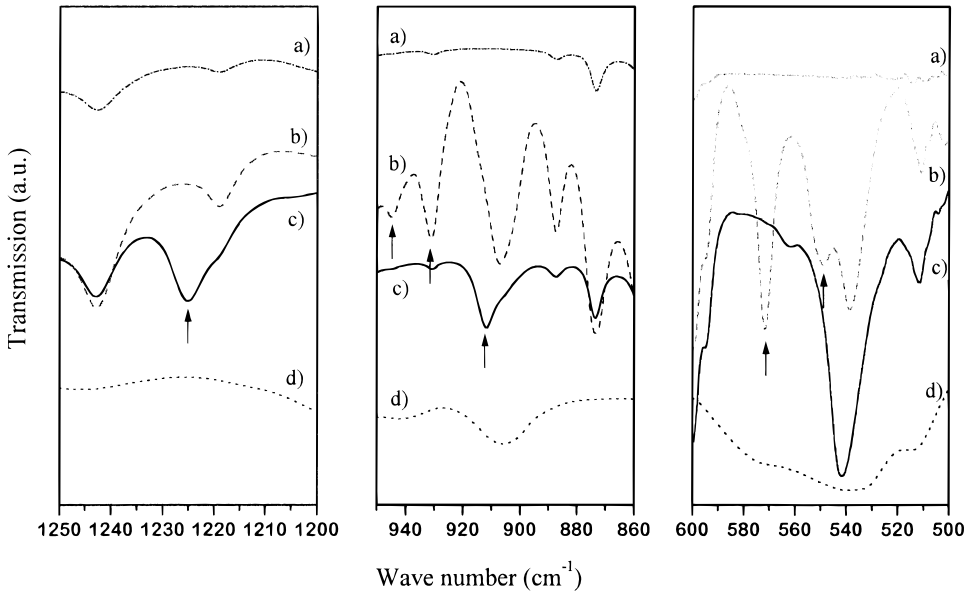

Figure 7. IR spectra of (a) pure *cis*-decalin, (b) the helical and (c) the zigzag conformations, and (d) amorphous sPS.

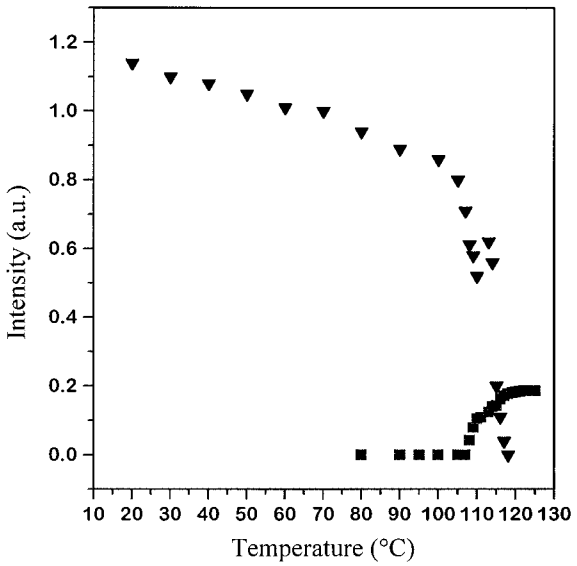

Figure 8. Evolution of the intensity of two typical bands during heating the sPS/*cis*-decalin solution: (▼) 572 cm^{-1} (helix) and (■) 1224 cm^{-1} (zigzag).

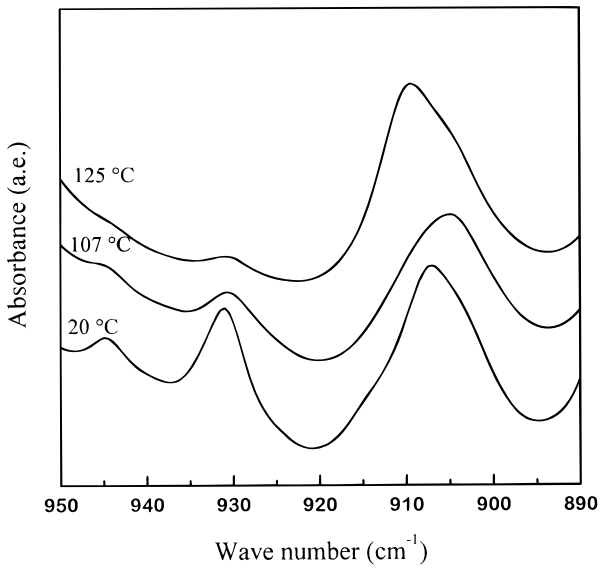

Figure 9. IR spectra during heating.

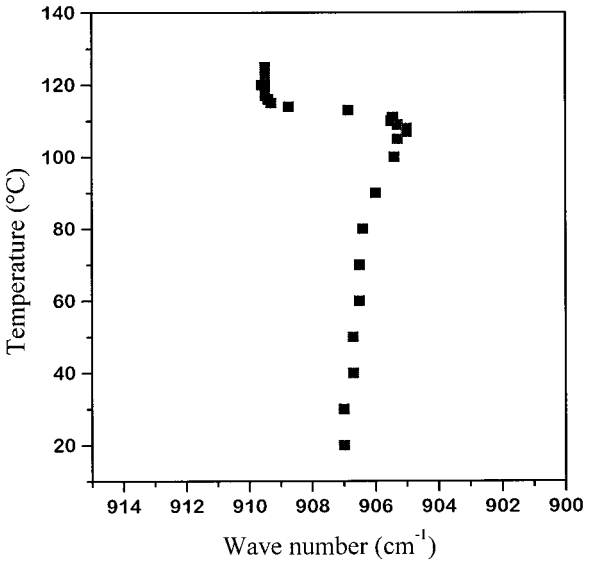

Figure 10. Evolution of the position of the IR absorption maximum in the region 900−910 cm^{-1} during heating.

melt in liquid nitrogen. The spectrum of the zigzag modification was recorded with a solution of $w_2 = 0.10$ from which the polymer was crystallized 120 °C. In the phase diagram (Figure 1), this temperature is situated at the border of the stability domain of the helical and zigzag phase. Only the zigzag phase is expected to be formed, as the formation of the helix phase necessitates a large degree of undercooling. In Figure 7c, the absorption at 1224.5 cm^{-1} is characteristic of the zigzag phase, but this absorption cannot be used to differentiate between the α- and β-phase. The absorption between 900 and 910 cm^{-1} can be used for this purpose. In this wave number range, three different signals can be observed. The absorption at 905.5 cm^{-1} is characteristic for the atactic isomer and amorphous sPS (7d). The signal shifts to 902.5 and 911 cm^{-1} for respectively the α- and β-phase.[31] The spectrum represented in Figure 7c clearly indicates the one is dealing with the β-phase. The spectrum of the helical phase (Figure 7b) was recorded with a sample that was quenched from the solution state in an ice bath. This conformation does not absorb in the wave number range from 1250 to 1200 cm^{-1}, but characteristic bands appear at 943, 572, and 548 cm^{-1}.

These IR characteristics were used in this study for the identification of the conformational transition from helix to zigzag. The sample was heated in the IR equipment in order to perform a dynamic measurement similar to the calorimetric and X-ray scattering experiments reported above. The most important changes take place between 100 and 120 °C. The evolution of the intensity of two typical bands is shown in Figure 8. The intensity of the band at 572 cm^{-1} is representative of the quantity of helical phase. The band at 1224.5 cm^{-1} represents the zigzag phase. A dramatic drop in the intensity of the band at 572 cm^{-1} sets in at 105 °C. This is followed by a sharp increase at 1224.5 cm^{-1}. At the same time, an increase of the intensity of the amorphous bands at 1155 and 1025 cm^{-1} takes place. The increase of the amorphous fraction indicates that the transition of the helix to zigzag conformation consists of a melting−recrystallization transition.

Also the change in the position of the absorption maximum in the region 905−911 cm^{-1} is remarkable. A few spectra at different temperatures are selected in Figure 9. The spectrum at 20 °C shows an absorption maximum at 907 cm^{-1}, and a shoulder at smaller wave numbers. At 107 °C, the temperature at which the melting of the helical phase sets in, the absorption maximum is positioned at this lower wave number but then shifts to a higher wave number to 910 cm^{-1} with increasing temperature. A shoulder at lower wave numbers is still present.

This continuous shift in the maxima is shown in Figure 10. The absorption maximum is observed at 907 cm^{-1} up to 95 °C but shifts to 905 cm^{-1} on further heating. Around 110 °C this absorption shifts back to the higher value of 910 cm^{-1}.

This final shift to 910 cm^{-1} clearly must be attributed to the formation of the β zigzag phase, and this confirms the earlier reported observations on the phase transformations. The shift to lower wave numbers in the temperature domain between 95 and 107 °C must be attributed to the intermediate formation of a less ordered phase. This can be an amorphous phase, having a maximum at 905.5 cm^{-1} (Figure 7d), or one of the mesomorphous phases described in literature. Auriemma et al. reported a mesophase having chains in

zigzag conformation with a characteristic IR-maximum at 903.5 cm^{-1} and a band at 1224 cm^{-1} related to the sequences in the trans-planar conformation.[23] This last observation, however, is absent in our spectra, so that it seems more probable that the shift to lower wave numbers of the band at 910 cm^{-1} results from the transition from the δ- to the β-phase through the amorphous phase. These observations also support the proposed mechanism of melting and recrystallization.

Conclusion

In *cis*-decalin, the helical phase (δ) is formed when a solution is quenched. On heating, this helix phase transforms into the zigzag phase (β) by a mechanism of melting−recrystallization. The earlier anticipated melting[25] of the thermodynamically less stable helical state and recrystallization into the stable planar zigzag phase has been observed with DSC, X-ray scattering, and FTIR. During this transformation, the metastable, incongruently melting compound (δ-phase) changes into the more stable crystal phase (β-phase).

Acknowledgment. Financial support by the National Fund for Scientific Research, the Interuniversity Poles of Attraction, Belgian State, Prime Ministers Office, Federal Office for Scientific, Technical, and Cultural Affairs (IUAP IV-P4/11), and the Flemish Institute for the Promotion of Scientific-Technological Research in Industry (IWT) for a fellowship to T.R. are gratefully acknowledged. S.R. wishes to acknowledge the Netherlands Organisation for Scientific Research (NWO) for research and travel grants.

References and Notes

(1) Vittoria, V.; Russo, R.; de Candia, F. *J. Macromol. Sci., Phys.* **1989**, *B28*, 419.
(2) Vittoria, V.; Filho, A.; de Candia, F. *J. Macromol. Sci., Phys.* **1990**, *B29*, 411.
(3) De Rosa, C.; Guerra, G.; Petraccone, V.; Corradini, P. *Polym. J.* **1991**, *23*, 12, 1435.
(4) Vittoria, V.; Filho, A.; de Candia, F. *J. Macromol. Sci., Phys.* **1991**, *B30*, 155.
(5) de Candia, F.; Filho, A.; Vittoria, V. *Colloid Polym. Sci.* **1991**, *269*, 650.
(6) De Rosa, C.; Rapacciuolo, M.; Guerra, G.; Petraccone, V.; Corradini, P. *Polymer* **1992**, *33*, 1423.
(7) Vittoria, V.; Filho, A.; de Candia, F. *J. Macromol. Sci., Phys.* **1992**, *B31*, 133.
(8) Chatani, Y.; Shimane, Y.; Ijitsu, T.; Yukinari, T. *Polymer* **1993**, *34*, 1625.
(9) Sun, Z.; Miller, R. *Polymer* **1993**, *34*, 1963.
(10) Vittoria, V.; de Candia, F.; Ianelli, P.; Immirzi, A. *Makromol. Chem., Rapid Commun.* **1988**, *9*, 765.
(11) Immirzi, A.; de Candia, F.; Ianelli, P.; Zambelli, A. *Makromol. Chem., Rapid Commun.* **1988**, *9*, 761.
(12) Guerra, G.; Vitagliano, V.; De Rosa, C.; Petraccone, V.; Corradini, P. *Macromolecules* **1990**, *23*, 1539.
(13) Kobayashi, M.; Nakaoki, T.; Ishihara N. *Macromolecules* **1989**, *22*, 4377.
(14) Chatani, Y.; Shimane, Y.; Inoue, Y.; Inagaki, T.; Ishioka, T.; Ijitsu, T.; Yukinari T. *Polymer* **1992**, *33*, 488.
(15) Prasad, A.; Mandelkern, L. *Macromolecules* **1990**, *23*, 5041.
(16) de Candia, F.; Romano, G.; Russo, R.; Vittoria, V. *Colloid Polym. Sci.* **1993**, *271*, 454.
(17) Chatani, Y.; Shimane, Y.; Inagaki, T.; Ijitsu, T.; Yukinari, T.; Shikuma, H. *Polymer* **1993**, *34*, 1620.
(18) de Candia, F.; Guadagno, G.; Vittoria, V. *J. Macromol. Sci., Phys.* **1994**, *B33*, 347.
(19) Kobayashi, M.; Yoshioka, T.; Kozasa, T.; Tashiro, K.; Suzuki, J.; Funahashi, S.; Izumi, Y. *Macromolecules* **1994**, *27*, 1349.
(20) Manfredi, C.; De Rosa, C.; Guerra, G.; Rapacciuolo, M.; Auriemma, F.; Corradini, P. *Macromol. Chem. Phys.* **1995**, *196*, 2795.
(21) de Candia, F.; Filho, A.; Vittoria, V. *Makromol. Chem., Rapid Commun.* **1991**, *12*, 295.
(22) Petraccone, V.; Auriemma. F.; Dal Poggetto, F.; De Rosa, C.; Guerra, G.; Corradini. P. *Makromol. Chem.* **1993**, *194*, 1335.
(23) Auriemma, F.; Petraccone, V.; Dal Pogetto, F.; De Rosa, C.; Guerra, G.; Manfredi, C.; Corradini, P. *Macromolecules* **1993**, *26*, 3772.
(24) de Candia, F.; Guadagno, G.; Vittoria, V. *J. Macromol. Sci., Phys.* **1995**, *B34*, 273.
(25) Deberdt, F.; Berghmans, H. *Polymer* **1993**, *34*, 2192.
(26) Deberdt, F.; Berghmans, H. *Polymer* **1994**, *35*, 1694.
(27) Roels, T.; Deberdt, F.; Berghmans, H. *Macromolecules* **1994**, *27*, 6216.
(28) Berghmans, H.; Deberdt, F. *Philos. Trans. R. Soc. London* **1994**, *398*, 117.
(29) Guenet, J. M.; Lotz, B.; Wittman, J. C. *Macromolecules* **1985**, *18*, 420.
(30) Kobayashi, M.; Nakaoki, T.; Ishihara, N. *Macromolecules* **1989**, *22*, 4377.
(31) Vittoria, V. *Polym Commun.* **1990**, *31*, 263, 2111.
(32) Guerra, G.; Musto, P.; Karasz, F.; MacKnight, W. *Makromol. Chem.* **1990**, *191*, 2111.
(33) Kobayashi, M.; Nakaoki, T. *Macromolecules* **1990**, *23*, 78.
(34) Reynolds, N.; Hsu, S. *Macromolecules* **1990**, *23*, 3463.
(35) Reynolds, N.; Stidham, H.; Hsu, S. *Macromolecules* **1991**, *24*, 3662.
(36) Kobayashi, M.; Kozasa, T. *Appl. Spectrosc.* **1993**, *47*, 1417.
(37) Su, Z.; Li, X.; Hsu, S.; *Macromolecules* **1994**, *27*, 287.

MA9707953